

Beyond Diagonal RIS: Passive Maximum Ratio Transmission and Interference Nulling Enabler

Hamad Yahya, *Member, IEEE*, Hongyu Li, *Graduate Student Member, IEEE*,
Matteo Nerini, *Graduate Student Member, IEEE*, Bruno Clerckx, *Fellow, IEEE*,
and Merouane Debbah, *Fellow, IEEE*

Abstract—Beyond diagonal reconfigurable intelligent surfaces (BD-RIS) generalizes and goes beyond conventional diagonal reconfigurable intelligent surfaces (D-RIS) by interconnecting elements to generate beyond diagonal scattering matrices, which significantly strengthen the wireless channels. In this work, we use BD-RIS for passive multiuser beamforming in multiuser multiple-input-single-output (MU-MISO) systems. Specifically, we design the scattering matrix of BD-RIS to either maximize the sum received signal power at the users following maximum ratio transmission (MRT), or to nullify the interference at the users following zero forcing (ZF). Furthermore, we investigate uniform/optimized power allocation and ZF precoding at the base station (BS). Numerical results show that BD-RIS improves the interference nulling capability and sum rate with fewer reflecting elements (REs) compared to D-RIS. In addition, at moderate to high signal to noise ratios (SNRs), passive interference nulling reduces the complexity at the BS by relaxing the need for precoding or water-filling power allocation design. Furthermore, the passive MRT with ZF precoding achieves a tight sum rate performance to the joint design considering MU-MISO scenarios with many REs while maintaining low computational complexity and simplifying the channel estimation.

Index Terms—Beyond diagonal reconfigurable intelligent surfaces (BD-RIS), multiuser beamforming, maximum ratio transmission (MRT), zero forcing (ZF).

I. INTRODUCTION

INTELLIGENT surfaces such as reconfigurable intelligent surfaces (RIS), also known as intelligent reflecting surfaces (IRS), are emerging technologies for the sixth generation (6G) mobile networks [1], and have recently been introduced to complement active relays [2], [3]. Unlike active relays, RIS is nearly-passive and noiseless, only powering the controller which alters the electrical properties of the reflecting elements (REs) by controlling the impedances attached to it [4]. Benefiting from its passiveness and reconfigurability, RIS has been recognized as a power-efficient enabler to engineer the wireless channel and enhance the communication performance by manipulating the phase and amplitude of the impinging signals without active circuitry and radio-frequency (RF) chains [5].

Hamad Yahya is with the Department of Electrical Engineering, Khalifa University of Science and Technology, Abu Dhabi 127788, UAE (email: hamad.myahya@ku.ac.ae), he is also with the Department of Electrical and Electronic Engineering, Imperial College London, London SW7 2AZ, U.K.

Hongyu Li, Matteo Nerini and Bruno Clerckx are with the Department of Electrical and Electronic Engineering, Imperial College London, London SW7 2AZ, U.K., (e-mail: {c.li21, m.nerini20, b.clerckx}@imperial.ac.uk).

Merouane Debbah is with the 6G Research Center, Khalifa University of Science and Technology, Abu Dhabi 127788, UAE (email: merouane.debbah@ku.ac.ae)

A. Related Work

RIS technologies have gained significant attention recently due to their potential to enhance the communication performance of wireless systems. Among these technologies, two prominent categories have been intensively investigated in the literature, which are diagonal reconfigurable intelligent surfaces (D-RIS) [6]–[12] and beyond diagonal reconfigurable intelligent surfaces (BD-RIS) [13]–[21]. While these two categories are often discussed separately, it is important to note that BD-RIS can be viewed as a generalization of D-RIS. In other words, BD-RIS encompasses the characteristics of D-RIS as a special case, offering a broader and more flexible framework for reconfigurable intelligent surfaces. The key limitation in D-RIS is that it manipulates only the phase of the incident signal with N impedances attached to N REs making it single-connected. In contrast, BD-RIS manipulates both the phase and amplitude of the incident signal with a network of impedances that connect the N REs together [13], [14]. By interconnecting all the REs to each other through $\frac{N(N+1)}{2}$ impedances, the fully-connected BD-RIS has been proposed, having the highest flexibility yet the highest circuit complexity. To balance BD-RIS circuit complexity and performance, group-connected architecture is introduced [13]. Also, graph theory is utilized to design optimal lower complexity architectures such as forest-connected and tree-connected [15]. While the above architectures are realized by reciprocal impedance networks, non-diagonal reconfigurable intelligent surfaces (ND-RIS) are proposed in [16] based on non-reciprocal impedance networks to increase the effective channel gain by ordering the channel gains in both directions.

Focusing on various RIS architectures, in existing literature, beamforming design for both D-RIS [6]–[12] and BD-RIS [16]–[21] aided multiuser multiple-input-single-output (MU-MISO) systems have been studied and explained in detail below.

D-RIS: The authors of [6] minimize the transmit power at the base station (BS) while maintaining a certain signal to interference and noise ratio (SINR) level at the users by jointly optimizing the scattering matrix of D-RIS and the active precoder at the BS using the alternating optimization (AO) algorithm. Similarly, Yang *et al.* [7] achieve the same goal using passive maximum ratio transmission (MRT)/zero forcing (ZF) at the D-RIS while iteratively optimizing the power allocation at the BS. Considering the same setup, the authors of [8] use AO framework to maximize the minimum rate for a better user fairness. The authors of [9] derive a closed-form steering vectors-based multiuser linear precoder to null the

known interference and minimize the unknown interference. Jiang *et al.* [10] use the AO framework to design the scattering matrix for interference nulling, achieving maximum degrees-of-freedom with high probability when the number of REs is $N > 2K(K - 1)$, with K the number of users. The authors of [11] present a robust gradient-based meta-learning approach without pre-training to design the scattering matrix and the BS precoding matrix. Jangsher *et al.* [12] maximize the sum rate of a wireless unmanned aerial vehicle (UAV) with RIS considering energy efficiency constraints and practical limitations such as phase compensation and imperfect channel state information (CSI).

BD-RIS: A two-stage design for the BD-RIS scattering matrix and BS precoding matrix is considered in [16], [17], unlike [18] which considers the joint design. For instance, Li *et al.* [16] consider ND-RIS with single-connected architecture and design the ND-RIS scattering matrix to maximize sum of the users' combined channel gain following semi-define relaxation method, while the popular water-filling method is used for power allocation although interference has not been nullified. Similarly, Fang and Mao [17] consider BD-RIS with group/fully-connected architectures and derive a closed-form BD-RIS scattering matrix to maximize the sum of the users' equivalent channel gains following the gradient decent approach and symmetric unitary projection, while regularized ZF precoding is considered at the BS. While relaxing the symmetry condition, the authors of [18] consider maximizing the sum rate and transforming the original problem into a multi-block optimization using auxiliary variables and solving it iteratively until convergence. In [19], Nerini *et al.* derive a closed-form BD-RIS scattering matrix that maximizes the channel gain of the single-user single-input-single-output (SISO) scenario and the solution is extended to the MU-MISO scenario. Furthermore, BD-RIS has been utilized in integrated sensing and communication (ISAC) systems [20], [21]. For instance, the authors of [20] jointly optimize the BS linear filter, and precoder, as well as the BD-RIS scattering matrix to maximize the sum rate while satisfying the sensing requirements. Chen and Mao [21] propose a two-stage design to jointly maximize the sum rate and minimize the largest eigenvalue of the Cramér-Rao bound matrix for multiple sensing targets.

B. Motivations and Contributions

Although a local optimal joint design was proposed in [18], the associated computational complexity of the proposed solution is significant. Therefore, a lower complexity two-stage design is proposed for multiuser systems in [16], [17]. Nonetheless, the focus in [16], [17], [19] is primarily on designing the BD-RIS scattering matrix to maximize the norm of the equivalent channel gains while the inter-user interference is neglected, and thus results in performance loss. Hence, it is more suitable for the point-to-point systems [22]. Therefore, this article focuses on efficiently and effectively addressing the interference management issue in multiuser systems by exploiting the interference management capability at fully-connected BD-RIS. The contributions of this work can be summarized as follows:

- 1) A two-stage design is considered for the BD-RIS scattering matrix and the BS precoding. Specifically, we analyze the received SINR at stage 1. We then design the BD-RIS scattering matrix to either maximize the sum received signal powers at the users following MRT structure, known as *passive MRT*, or to nullify the interference following ZF structure, known as *passive interference nulling*.
- 2) Closed-form BD-RIS scattering matrix expressions are presented for the passive MRT following the symmetric unitary projection [17], while an efficient AO algorithm is presented for the passive interference nulling. It is found that applying the symmetric unitary projection improves the received SINR at stage 1 for the passive MRT.
- 3) For stage 2, we consider uniform/optimized power allocation and ZF precoding at the BS. Specifically, the optimized power allocation aims to maximize the sum rate while the BD-RIS scattering matrix is given. For instance, passive MRT requires optimization to achieve sum rate maximization, meanwhile when the passive interference nulling is adopted at the BD-RIS, water-filling power allocation is applied at the BS. On the other hand, ZF precoding at the BS is proposed for the passive MRT.
- 4) The computational complexity for both stages is analyzed considering the two BD-RIS designs and the BS processes. In addition, the channel state information requirements for each design are specified. For instance, it is found that the passive MRT eases the channel state information requirements which further simplifies the channel estimation.
- 5) The numerical results show that the BD-RIS enhances the interference nulling capability compared to the D-RIS. For instance, BD-RIS can support more users simultaneously for the same number of REs. Also, the algorithm for BD-RIS converges rapidly with a smaller number of iterations and have a more stable interference nulling regardless of the initialization value.

C. Article Organization

The rest of the article is organized as follows. Sec. II introduces the system and channel models of the BD-RIS-enabled MU-MISO systems. Sec. III is the BD-RIS scattering matrix design for passive MRT and interference nulling. Sec. IV is the BS power allocation/precoding design. Sec. V is the numerical results and discussions. Finally, Sec. VI concludes the article with the main remarks and future work.

D. Notations

The notations used throughout the paper are explained as follows. Boldface uppercase and lowercase symbols such as \mathbf{X} and \mathbf{x} will denote matrix and column vectors, respectively. The matrix Kronecker product symbol is \otimes . The transpose, Hermitian transpose, complex conjugate and Moore-pseudoinverse are denoted by $(\cdot)^T$, $(\cdot)^H$, $(\cdot)^*$ and $(\cdot)^\dagger$. Also, $(x)^+ = \max(x, 0)$, $\lceil \cdot \rceil$ is the ceiling function, $\mathbb{E}[\cdot]$ is the statistical expectation, $\text{Re}[\cdot]$ is the real value of a complex

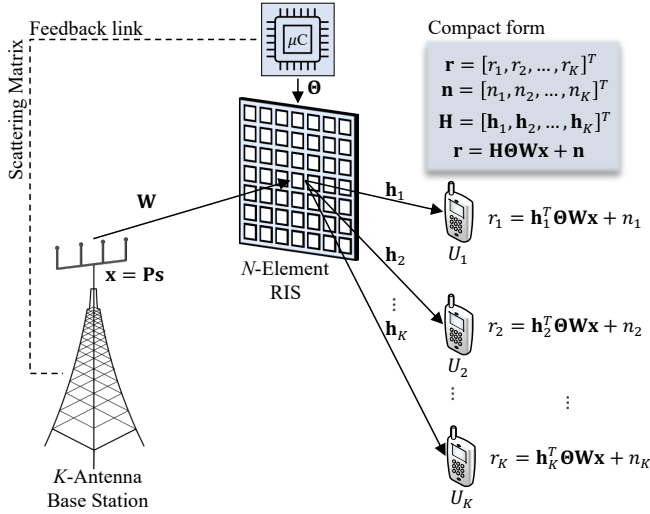


Fig. 1. System block diagram.

number, $|\cdot|$ is the absolute value, $\|\cdot\|_2$ is the l^2 norm, $\|\cdot\|_F$ is the Frobenius norm, $\text{Tr}(\cdot)$ is the trace, $[\mathbf{X}]_{i,j}$ is i -th row and j -th column entry in \mathbf{X} , $[\mathbf{x}]_i$ is i -th entry in \mathbf{x} . The identity matrix and zeros vectors are denoted as \mathbf{I} and $\mathbf{0}$, respectively. In addition, $\text{vec}(\mathbf{X})$ is the matrix vectorization process which concatenate the columns of the matrix in one column vector, while $\text{reshape}(\mathbf{x}, [a, b])$ reshapes the vector to an $a \times b$ matrix. The complex normal random variable with a zero mean and σ^2 variance is denoted as $\mathcal{CN}(0, \sigma^2)$.

II. SYSTEM AND CHANNEL MODELS

In a downlink MU-MISO system, the BS is equipped with K transmit antennas to serve K single antenna users through a fully-connected BD-RIS with N REs. The precoded signal vector to be transmitted at the antenna ports of the BS can be expressed as $\mathbf{x} = \mathbf{P}\mathbf{s}$, where $\mathbf{s} \in \mathbb{C}^{K \times 1}$ is the information symbols vector with $\mathbb{E}[\mathbf{s}\mathbf{s}^H] = \mathbf{I}$, and the precoding matrix is denoted by $\mathbf{P} \in \mathbb{C}^{K \times K}$ such that $\|\mathbf{P}\|_F^2 = P_{\max}$ with P_{\max} the maximum transmission power at the BS. Let the k th user be denoted as U_k , $k \in \{1, 2, \dots, K\}$, the received signal at U_k is expressed as

$$r_k = \mathbf{h}_k^T \Theta \mathbf{W} \mathbf{x} + n_k \quad (1)$$

where $\mathbf{W} \in \mathbb{C}^{N \times K}$ is the BS-BD-RIS channel matrix, $\Theta \in \mathbb{C}^{N \times N}$ is the BD-RIS scattering matrix, $\mathbf{h}_k \in \mathbb{C}^{N \times 1}$ is BD-RIS- U_k channel vector, and $n_k \sim \mathcal{CN}(0, N_0)$ is the additive white Gaussian noise (AWGN) with N_0 the power spectral density. In addition, Θ belongs to the complex unitary symmetric set due to its lossless and reciprocal impedance network, i.e., $\Theta \in \mathcal{S}_{\text{loss}} = \{\Theta | \Theta \Theta^H = \mathbf{I}\}$ and $\Theta \in \mathcal{S}_{\text{recip}} = \{\Theta | \Theta = \Theta^T\}$ [13]. It is worth noting that the BS- U_k channel is assumed to be blocked to highlight the performance gain of the BD-RIS [19]. To allow a systematic design of the scattering matrix, (1) can be written in a compact form such that the received signal vector is $\mathbf{r} = \mathbf{H} \Theta \mathbf{W} \mathbf{x} + \mathbf{n} \in \mathbb{C}^{K \times 1}$, where $\mathbf{H} = [\mathbf{h}_1, \dots, \mathbf{h}_K]^T \in \mathbb{C}^{K \times N}$ is the concatenated BD-RIS- U_k , $\forall k$ channel matrix, and \mathbf{n} is the AWGN vector with independent and identically distributed (i.i.d) entries. Fig. 1 depicts the system block diagram.

While Θ and \mathbf{P} are given, the received SINR at U_k is

$$\gamma_k = \frac{|\mathbf{h}_k^T \Theta \mathbf{W} \mathbf{p}_k|^2}{\sum_{i \neq k} |\mathbf{h}_k^T \Theta \mathbf{W} \mathbf{p}_i|^2 + N_0} \quad (2)$$

Consequently, sum rate maximization problem is formulated as

$$(P1) : \max_{\mathbf{P}, \Theta} \sum_k \log_2(1 + \gamma_k) \quad (3a)$$

$$\text{Subject to,} \quad \|\mathbf{P}\|_F^2 = P_{\max} \quad (3b)$$

$$\Theta = \Theta^T \quad (3c)$$

$$\Theta \Theta^H = \mathbf{I} \quad (3d)$$

The objective function in (P1) shows a strong coupling between the precoding matrix and the scattering matrix, which makes it difficult to jointly optimize two matrices. Therefore, it is suggested to have a two-stage design. Unlike [17], our proposed design directly enhances the SINR by applying passive MRT/interference nulling at the BD-RIS. Such approach is motivated by the fact that utilizing ZF solely at the BS usually incurs power penalty because most of the power is wasted for channel inversion, resulting in having very small power gains [23]. Hence, due to the BD-RIS passive nature, enhancing the SINR by the BD-RIS is more effective than relying solely on the BS for precoding.

III. STAGE 1: BD-RIS SCATTERING MATRIX DESIGN

To explore to what extent BD-RIS could help to enhance the sum rate performance in (3a), we fix the impact of the BS precoding by setting $\mathbf{P} = \sqrt{p_k} \mathbf{I}$, where $p_k = \frac{P_{\max}}{K}$, $\forall k$. Hence, the received signal vector can be written as

$$\mathbf{r} = \sqrt{p_k} \mathbf{H} \Theta \mathbf{W} \mathbf{s} + \mathbf{n} \triangleq \sqrt{p_k} \mathbf{H} \Omega \mathbf{s} + \mathbf{n} \triangleq \sqrt{p_k} \mathbf{E} \mathbf{s} + \mathbf{n} \quad (4)$$

where $\Omega = \Theta \mathbf{W} = [\omega_1, \dots, \omega_K] \in \mathbb{C}^{N \times K}$ and the equivalent channel is $\mathbf{E} = \mathbf{H} \Omega = [\mathbf{e}_1, \dots, \mathbf{e}_K]^T \in \mathbb{C}^{K \times K}$. Consequently, the received SINR at U_k stage 1 is given as

$$\gamma_k = \frac{p_k |\mathbf{h}_k^T \omega_k|^2}{p_k \sum_{i \neq k} |\mathbf{h}_k^T \omega_i|^2 + N_0} = \frac{p_k |[\mathbf{e}_k]_k|^2}{p_k \sum_{i \neq k} |[\mathbf{e}_k]_i|^2 + N_0} \quad (5)$$

Considering (5), the rate at U_k is influenced by the signal power that is determined by the numerator, as well as the interference which is determined by the summation in the denominator. Therefore, two objectives for the BD-RIS are motivated:

- 1) To maximize the desired signal power.
- 2) To nullify the interference.

The BD-RIS scattering matrix design following the first objective is called *passive MRT*, while the design following the latter is called *passive interference nulling*. It is worth noting that maximizing $\|\mathbf{E}\|_F^2$ as in [17] would maximize $\sum_k \sum_i |[\mathbf{e}_k]_i|^2$. Hence, the numerator and denominator of (5) are maximized simultaneously, which does not necessarily lead to the maximization of the SINR in a MU-MISO setting.

A. Passive MRT

To maximize the desired signal power at all users simultaneously, the diagonal elements of \mathbf{E} need to be considered, i.e., $[e_k]_k$. Following the approach in [24], it is noted that ω_k and $\exp(j\theta_k)\omega_k$ for any common phase rotation $\theta_k \in \mathbb{R}$ lead to the same values of $|[e_k]_k|$. Hence, the phase ambiguity can be exploited to make the inner product $\mathbf{h}_k^T \omega_k$ real and positive without loss of optimality. This motivates us to maximize the real part of $\mathbf{h}_k^T \omega_k$ instead of its absolute value. Therefore, to capture the desired signal at all users, the trace of the real-valued equivalent channel will be used while relaxing the challenging unitary and symmetric constraints. Consequently, we can find a relaxed Θ by solving the following problem

$$(P2a) : \max_{\Theta} f(\Theta) \triangleq \text{Tr}(\text{Re}[\mathbf{E}]) = \text{Tr}(\text{Re}[\mathbf{H}\Theta\mathbf{W}]) \quad (6a)$$

$$\text{Subject to, } \|\Theta\|_F^2 = N \quad (6b)$$

The objective function can be written as $f(\Theta) = \text{Tr}(\text{Re}[\mathbf{E}]) = \frac{1}{2}(\text{Tr}(\mathbf{E}) + \text{Tr}(\mathbf{E}^*)) = \frac{1}{2}(\text{Tr}(\mathbf{E}) + \text{Tr}(\mathbf{E}^*)) = \text{Re}[\text{Tr}(\mathbf{E})]$. Hence, $f(\Theta) = \text{Tr}(\text{Re}[\mathbf{H}\Theta\mathbf{W}]) = \text{Re}[\text{Tr}(\mathbf{H}\Theta\mathbf{W})]$. Using the cyclic property of the trace, we can write the objective function in (6a) as $f(\Theta) = \text{Re}[\text{Tr}(\mathbf{G}\Theta)]$, where $\mathbf{G} = \mathbf{W}\mathbf{H} \in \mathbb{C}^{N \times N}$ is the cascaded BS-BD-RIS- U_k channel matrix. By expanding the trace and the Frobenius norm, the optimization problem can be written as

$$(P2a) : \max_{\Theta} f(\Theta) = \text{Re} \left[\sum_{i=1}^N \sum_{j=1}^N [\mathbf{G}]_{i,j} [\Theta]_{j,i} \right] \quad (7a)$$

$$\text{Subject to, } \sum_{i=1}^N \sum_{j=1}^N |[\Theta]_{j,i}|^2 = N \quad (7b)$$

The objective function in (7a) can be maximized by co-phasing the terms $[\mathbf{G}]_{i,j}$ and $[\Theta]_{j,i}$ before summation. Such problem has a closed-form solution that follows the MRT precoding [25] and the pseudo match-and-forward precoding for non-regenerative multiple-input-multiple-output (MIMO) relays [26]. Hence, the solution of (P2a) is expressed as

$$[\Theta]_{j,i} = [\mathbf{G}]_{i,j}^* \sqrt{\frac{N}{\text{Tr}(\mathbf{G}\mathbf{G}^H)}} \quad (8)$$

where the normalization factor is used to satisfy the constraint in (6b). Therefore, in a matrix form, the low-complexity Θ can be expressed as

$$\Theta = \mathbf{G}^H \sqrt{\frac{N}{\text{Tr}(\mathbf{G}\mathbf{G}^H)}} \quad (9)$$

Since (9) does not belong to the feasible set and violates the lossless and reciprocal BD-RIS constraints, i.e., $\Theta\Theta^H = \mathbf{I}$ and $\Theta = \Theta^T$; we formulate an optimization problem to find Θ which belongs to the feasible set by minimizing the squared

Frobenius distance between the low-complexity Θ and the desired Θ . Hence,

$$(P2b) : \Theta^* = \arg \min_{\Theta} \left\| \Theta - \mathbf{G}^H \sqrt{\frac{N}{\text{Tr}(\mathbf{G}\mathbf{G}^H)}} \right\|_F^2 \quad (10a)$$

$$\text{Subject to, (3c), (3d)} \quad (10b)$$

Such approach is known as a matrix approximation and is used due to its ease of computation. In addition, the squared Frobenius norm is used specifically because it is reported that it maximizes the entropy for quantized channels in MIMO systems [27]. This problem can be solved efficiently following [17, Eq. (10)-(12)], which projects the low-complexity solution to the feasible set, i.e., (9) needs symmetric unitary projection. The symmetric projection of Θ is given as [17, Eq. (10)],

$$\Pi_{\mathcal{S}_{\text{recip}}}(\Theta) = 0.5(\Theta + \Theta^T) \quad (11)$$

The unitary projection of Θ is given as [17, Eq. (11)],

$$\Pi_{\mathcal{S}_{\text{loss}}}(\Theta) = \mathbf{U}\mathbf{V}^H \quad (12)$$

where its singular value decomposition (SVD) can be written as $\Theta = \mathbf{U}\Sigma\mathbf{V}^H$, \mathbf{U} and \mathbf{V} are the unitary left and right singular vectors and Σ contains the singular values ordered in a descending order. Finally, the unitary projection of $\Pi_{\mathcal{S}_{\text{recip}}}(\Theta)$ is given as [17, Eq. (12)],

$$\Pi_{\mathcal{S}_{\text{loss}}}(\Pi_{\mathcal{S}_{\text{recip}}}(\Theta)) = \hat{\mathbf{U}}\mathbf{V}^H \quad (13)$$

where $\Pi_{\mathcal{S}_{\text{recip}}}(\Theta)$ is a rank deficient matrix with rank R and its unitary left and right singular vectors are $\mathbf{U} = [\mathbf{U}_R, \mathbf{U}_{N-R}]$ and $\mathbf{V} = [\mathbf{V}_R, \mathbf{V}_{N-R}]$. Also, $\hat{\mathbf{U}} = [\mathbf{U}_R, \mathbf{V}_{N-R}^*]$. Finally, we can express the optimal scattering matrix in closed-form as

$$\Theta^* = \Pi_{\mathcal{S}_{\text{loss}}} \left(\Pi_{\mathcal{S}_{\text{recip}}} \left(\mathbf{G}^H \sqrt{\frac{N}{\text{Tr}(\mathbf{G}\mathbf{G}^H)}} \right) \right) \quad (14)$$

It should be noted that the signal in general will be degraded due to the symmetric unitary projection.

It will be seen in the Numerical Results and Discussions Section that the symmetric unitary projection not only will degrade the signal power but also will reduce the interference power in (5).

Computational Complexity: The computational complexity of (14) depends on the complexity of (9), $\mathcal{O}(KN^2 + N^2)$, and is dominated by the SVD computation for (12), $\mathcal{O}(N^3)$. Hence, the overall complexity can be written as $\mathcal{O}(N^3 + KN^2 + N^2) = \mathcal{O}(N^3)$.

Channel State Information Requirements: Furthermore, the cascaded BS-BD-RIS- U_k channel matrix, \mathbf{G} , is needed to compute Θ^* . This can be found considering the single-connected architecture by selecting the inter-impedance elements of the BD-RIS to have an infinitely large reactance. Hence, \mathbf{G} can be estimated by setting $\Theta = \mathbf{I}$ [28] and the channel estimation is simplified without separately estimating \mathbf{H} and \mathbf{W} .

B. Passive Interference Nulling

To nullify the interference terms in (5), the equivalent channel should result in a diagonal matrix, i.e., $\mathbf{E} = \mathbf{H}\Theta\mathbf{W} = \text{diag}(\mathbf{\Lambda})$ and $\mathbf{\Lambda} \in \mathbb{C}^{K \times 1}$ is the interference-free equivalent channels at the users. An intuitive approach to design a low-complexity Θ that nulls the interference follows the ZF precoding. Hence,

$$\Theta = \mathbf{G}^\dagger \sqrt{\frac{N}{\text{Tr}(\mathbf{G}^{\dagger H} \mathbf{G}^\dagger)}} \quad (15)$$

where $\mathbf{G}^\dagger = \mathbf{H}^H (\mathbf{H}\mathbf{H}^H)^{-1} (\mathbf{W}^H \mathbf{W})^{-1} \mathbf{W}^H$ and the normalization factor is to satisfy the constraint in (6b). Nonetheless, (15) does not belong to the feasible set. Hence, the optimal unitary symmetric scattering matrix that is the closest to (15) in terms of Frobenius norm can be written in closed-form as $\Theta^* = \Pi_{\mathcal{S}_{\text{loss}}} \left(\Pi_{\mathcal{S}_{\text{recip}}} \left(\mathbf{G}^\dagger \sqrt{\frac{N}{\text{Tr}(\mathbf{G}^{\dagger H} \mathbf{G}^\dagger)}} \right) \right)$.

It is worth noting that the approximation error has a determinantal effect on the equivalent channel as \mathbf{E} will be no longer diagonal which is proved in the following.

Proof. While dropping the normalization factor in (15), the equivalent channel can be written as

$$\mathbf{E} = \mathbf{H}\mathbf{H}^\dagger \mathbf{W}^\dagger \mathbf{W} = \mathbf{I} \quad (16)$$

While we consider the symmetry condition alone to facilitate the proof, the equivalent channel becomes

$$\begin{aligned} \hat{\mathbf{E}} &= 0.5\mathbf{H}\mathbf{H}^\dagger \mathbf{W}^\dagger \mathbf{W} + 0.5\mathbf{H}\mathbf{W}^{\dagger T} \mathbf{H}^{\dagger T} \mathbf{W} \\ &= 0.5\mathbf{I} + 0.5\mathbf{H}\mathbf{W}^{\dagger T} \mathbf{H}^{\dagger T} \mathbf{W} \end{aligned} \quad (17)$$

which is in general not a diagonal matrix. \square

To effectively nullify the interference, we adopt an alternative approach as detailed below. The adopted approach is inspired by the interference nulling presented for D-RIS in [10]. Hence, to null the interference in a BD-RIS-enabled MU-MISO system, the equivalent channel, i.e., \mathbf{E} , needs to be classified into a desired/interference channels. The case is different for BD-RIS as the impinging wave on a certain RE can be also reflected by other REs due to the fully-connected nature of the BD-RIS. Therefore, we can re-write the equivalent channel as $\text{vec}(\mathbf{E}) = \text{vec}(\mathbf{H}\Theta\mathbf{W}) = \mathbf{A}\text{vec}(\Theta)$, where $\mathbf{A} = \mathbf{W}^T \otimes \mathbf{H} \in \mathbb{C}^{K^2 \times N^2}$ denotes the desired and interference channels matrix. For instance, $\mathbf{a}_i^T = [\mathbf{A}]_{i,:}$ represents the desired/interference channels for a specific user. We define $\tilde{\mathbf{a}}_{\hat{k},k} = \mathbf{a}_i$, for $i = (k-1) \times K + \hat{k}$. If $\hat{k} = k$, then $\tilde{\mathbf{a}}_{\hat{k},k}$ is the desired channel for U_k . Otherwise, $\tilde{\mathbf{a}}_{\hat{k},k}$ is the interference channel for U_k from antenna \hat{k} . Furthermore, the interference channels matrix can be defined as

$$\bar{\mathbf{A}} = [\bar{\mathbf{A}}_1, \bar{\mathbf{A}}_2, \dots, \bar{\mathbf{A}}_K] \in \mathbb{C}^{N^2 \times K(K-1)} \quad (18a)$$

$$\bar{\mathbf{A}}_1 = [\tilde{\mathbf{a}}_{2,1}, \tilde{\mathbf{a}}_{3,1}, \dots, \tilde{\mathbf{a}}_{K,1}] \quad (18b)$$

$$\begin{aligned} \bar{\mathbf{A}}_k &= [\tilde{\mathbf{a}}_{1,k}, \dots, \tilde{\mathbf{a}}_{k-1,k}, \tilde{\mathbf{a}}_{k+1,k}, \dots, \tilde{\mathbf{a}}_{K,k}], \\ &1 < k \leq K-1 \end{aligned} \quad (18c)$$

$$\bar{\mathbf{A}}_K = [\tilde{\mathbf{a}}_{1,K}, \tilde{\mathbf{a}}_{2,K}, \dots, \tilde{\mathbf{a}}_{K-1,K}] \quad (18d)$$

In addition, the desired channels matrix is defined as $\check{\mathbf{A}} = [\check{\mathbf{a}}_{1,1}, \check{\mathbf{a}}_{2,2}, \dots, \check{\mathbf{a}}_{K,K}] \in \mathbb{C}^{N^2 \times K}$. To achieve $\mathbf{E} = \text{diag}(\mathbf{\Lambda}) \Leftrightarrow$

$\mathbf{A}\text{vec}(\Theta) = \text{vec}(\text{diag}(\mathbf{\Lambda}))$, the $K(K-1)$ interference channels needs to be nulled by the BD-RIS. This can be achieved by satisfying the nulling condition, which is expressed as

$$\bar{\mathbf{A}}^T \text{vec}(\Theta) = \mathbf{0} \quad (19)$$

In general, (19) can be seen as a system of linear equations with $K(K-1)$ complex equations and N^2 complex variables. Nonetheless, the number of effective variables is less due to the symmetry and unitary conditions on Θ , which has effectively the diagonal elements and upper/lower triangle, that is, the number of effective variables is $\frac{N}{2}(1+N)$ real variable. Therefore, (19) can be achieved if the number of real variables is greater or equal the number of real equations, i.e., $\frac{N}{2}(1+N) \geq 2K(K-1)$. Therefore, by solving the quadratic inequality and noting that K and N are integers, we can write $N \geq \left\lceil \frac{-1 + \sqrt{16K^2 - 16K + 1}}{2} \right\rceil$ which is equivalent to $N \geq 2K-1$ for $K > 1$. This can be proved by showing that $\frac{-1 + \sqrt{16K^2 - 16K + 1}}{2}$ lies strictly between $2K-2$ and $2K-1$ for $K > 1$.

Therefore, by setting $N \geq 2K-1$, Θ that achieves (19) always exists. Such figure for N is way less compared to the D-RIS which requires at least $N > 2K(K-1)$ [10].

Consequently, the objective is to find Θ that is subject to the interference nulling, BD-RIS lossless and reciprocity conditions. In other words, we have the following feasibility-check problem

$$(P3) : \text{Find } \Theta \quad (20a)$$

$$\text{Subject to, (19), (3c), (3d)} \quad (20b)$$

Such problem is non-convex and challenging to solve. Therefore, AO is used to find Θ that complies with the previously mentioned constraints by projecting a certain initial solution into $\mathcal{S}_{\text{null}}$, $\mathcal{S}_{\text{loss}}$ and $\mathcal{S}_{\text{recip}}$ alternatively. Fortunately, the symmetric and unitary projections have been presented with closed-form solutions in (11)–(12), while the interference nulling projection follows [10, Eq. (21a)] such that

$$\Pi_{\mathcal{S}_{\text{null}}}(\Theta) = \text{reshape}(\mathbf{v}(\Theta), [N, N]) \quad (21)$$

where $\mathbf{v}(\Theta) = \text{vec}(\Theta) - \bar{\mathbf{A}}^* (\bar{\mathbf{A}}^T \bar{\mathbf{A}}^*)^{-1} \bar{\mathbf{A}}^T \text{vec}(\Theta) \in \mathbb{C}^{N^2 \times 1}$.

A pseudo-code that illustrates the steps to obtain Θ^* through AO is given in Algorithm 1. The algorithm needs the interference channels matrix $\bar{\mathbf{A}}$ as input. It starts by initializing the scattering matrix, which can be either a random initialization or a specific initialization. Furthermore, the initialized scattering matrix is projected to the lossless and reciprocal sets. Lines 3–8 illustrate the iterative AO which projects the Θ from the previous iteration to interference nulling set and the lossless and reciprocal sets. This continues for a certain number of iterations until the breaking condition on line 7 is met. On line 6, δ is computed which is the l^2 norm for the nulling condition difference between the current iteration and the previous iteration. Finally, the symmetric unitary Θ^* that achieves interference nulling is returned. It is worth noting that ϵ and ε determine the algorithm convergence speed, where the former is the relative rate of change tolerance and the latter is the nulling condition norm tolerance.

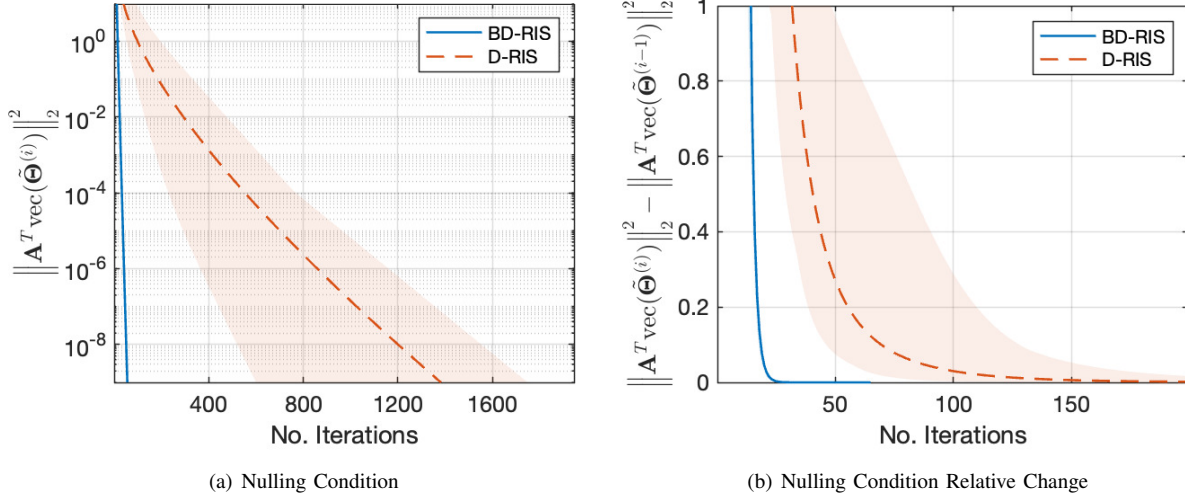


Fig. 2. Convergence vs. number of iterations for interference nulling using BD-RIS and D-RIS with random initialization, where $K = 8$ and $N = 144$. a) Nulling condition l^2 norm. b) Nulling condition l^2 norm relative change.

Algorithm 1: AO for passive interference nulling.

Input: $\bar{\mathbf{A}}$, Iter, ϵ , ε
Output: Θ^*

- 1 Initialize $\Theta^{(0)}$
- 2 $\tilde{\Theta}^{(0)} = \Pi_{\mathcal{S}_{\text{recip}}}(\Pi_{\mathcal{S}_{\text{loss}}}(\Theta^{(0)}))$
- 3 **for** $i = 1 : \text{Iter}$ **do**
- 4 $\Theta^{(i)} = \Pi_{\mathcal{S}_{\text{null}}}(\tilde{\Theta}^{(i-1)})$
- 5 $\tilde{\Theta}^{(i)} = \Pi_{\mathcal{S}_{\text{recip}}}(\Pi_{\mathcal{S}_{\text{loss}}}(\Theta^{(i)}))$
- 6 $\delta = \frac{\|\mathbf{A}^T \text{vec}(\tilde{\Theta}^{(i)})\|_2^2 - \|\mathbf{A}^T \text{vec}(\tilde{\Theta}^{(i-1)})\|_2^2}{\|\bar{\mathbf{A}}^T \text{vec}(\tilde{\Theta}^{(i-1)})\|_2^2}$
- 7 **if** $\delta \leq \epsilon$ **or** $\|\bar{\mathbf{A}}^T \text{vec}(\tilde{\Theta}^{(i)})\|_2^2 < \varepsilon$ **or** $i > \text{Iter}$ **then**
- 8 **break** and Go to Line 9
- 9 $\Theta^* = \tilde{\Theta}^{(i)}$

Fig. 2 compares the convergence of Algorithm 1 with the D-RIS interference nulling AO algorithm [10]. Random initialization is assumed for both, with $N = 144$, $K = 8$, $\epsilon = 10^{-6}$, $\varepsilon = 10^{-10}$, Iter = 10^4 , and 100 realizations are considered for Monte-Carlo simulation. Also, i.i.d Rayleigh fading channels are considered. The curves represent the average convergence of the algorithm over 10^4 iterations, while the shades represent the possible variations, i.e., the maximum and minimum convergence. It can be observed that BD-RIS achieves a rapid interference nulling, reaching 10^{-8} with significantly fewer iterations compared to D-RIS. In addition, the relative change for BD-RIS stabilizes after fewer iterations compared to D-RIS. Moreover, BD-RIS maintains a stable pattern, effectively achieving interference nulling, unlike D-RIS which is more dependent on the initialization of the scattering matrix, resulting in less stable interference nulling.

Computational Complexity: The computational complexity of Algorithm 1 is dominated by computing the projections inside the loop. For instance, in (21), its main part, i.e., $\bar{\mathbf{A}}^* (\bar{\mathbf{A}}^T \bar{\mathbf{A}}^*)^{-1} \bar{\mathbf{A}}^T$, can be computed outside

the loop as it only depends on the interference channels matrix. Hence, its computational complexity can be written as $\mathcal{O}(K^6 + K^2 N^4 + K^4 N^2 + K^2 N^2)$. In addition, the lossless and reciprocal projections inside the loop have a computational complexity of $\mathcal{O}(tN^3)$ and $\mathcal{O}(tN^2)$, where t is the number of iterations. Consequently, the overall algorithm's computational complexity is $\mathcal{O}(tN^3 + tN^2 + K^6 + K^2 N^4 + K^4 N^2 + K^2 N^2)$. If $N = 2K - 1$, the computational complexity can be written as $\mathcal{O}(K^6)$, otherwise if $N \gg K$, then the computational complexity can be written as $\mathcal{O}(K^2 N^4)$. Moreover, the Numerical Results and Discussions Section will show that initializing based on passive MRT solution, (14), improves the sum rate performance compared to the random initialization.

Channel State Information Requirements: The interference channels matrix $\bar{\mathbf{A}}$ is needed to compute Θ^* . This can be found by pre-designing the variation of Θ for the fully-connected BD-RIS architecture to be further used in the training process [29].

IV. STAGE 2: BS POWER CONTROL/PRECODING

As Θ^* is determined at stage 1, the precoding matrix \mathbf{P} relies only on the equivalent channel matrix, i.e., $\mathbf{E} = \mathbf{H}\Theta^*\mathbf{W}$ which is of low-dimension compared to the individual channel matrices. Hence, (3a) can be written as

$$(P4) : \max_{\mathbf{P}} \sum_k \log_2 \left(1 + \frac{|\mathbf{h}_k^T \Theta^* \mathbf{W} \mathbf{p}_k|^2}{\sum_{i \neq k} |\mathbf{h}_k^T \Theta^* \mathbf{W} \mathbf{p}_i|^2 + N_0} \right) \quad (22a)$$

$$\text{Subject to, (3b)} \quad (22b)$$

Solving this optimization problem for the general case is not straightforward. Therefore, a distinction is made between the passive MRT and interference nulling solutions.

A. Power Control/Precoding for Passive MRT

Since the passive MRT presented in Sec. III-A does not set the interference terms to zero, a low-complexity precoder can

be considered at the BS such as ZF. Consequently,

$$\mathbf{P} = \mathbf{E}^\dagger \sqrt{\frac{P_{\max}}{\text{Tr}(\mathbf{E}^\dagger \mathbf{H} \mathbf{E})}} \quad (23)$$

where the normalization factor ensures $\|\mathbf{P}\|_F^2 = P_{\max}$. The computational complexity of the ZF solution is bounded by the dimension of the equivalent channels matrix, and hence, it can be written as $\mathcal{O}(K^3)$.

Alternatively, employing simple power allocation approaches at the BS will ease the requirements of high resolution digital-to-analog converters [30]. In addition, the number of real variables will reduce to K , unlike the full precoder which has K^2 complex variables. Two power allocation approaches are devised, which are the uniform power and optimized power. The former considers equal power allocation among the signal vector elements, i.e.,

$$\mathbf{P} = \text{diag}(\sqrt{p_1}, \sqrt{p_2}, \dots, \sqrt{p_K}) \quad (24)$$

such that $p_k = \frac{P_{\max}}{K}, \forall k$. Hence, it is agnostic to the equivalent channels matrix. On the other hand, while the equivalent channels matrix is known at the BS, the optimized power can be designed to maximize the sum rate of the system. Therefore, the sum rate maximization problem can be formulated as [31, Eq. (3)],

$$(P5) : \max_{p_k} \sum_k \log_2 \left(1 + \frac{p_k |\mathbf{h}_k^T \Theta^* \mathbf{w}_k|^2}{\sum_{i \neq k} p_i |\mathbf{h}_k^T \Theta^* \mathbf{w}_i|^2 + N_0} \right) \quad (25a)$$

$$\text{Subject to,} \quad \sum_k p_k = P_{\max} \quad (25b)$$

$$p_k \geq 0 \quad (25c)$$

where (25a) is non-linear and non-convex, (25b) is affine and linear and (25c) defines a hyperplane and is convex. Such optimization problem can be solved efficiently using interior-point optimization algorithms.

B. Power Control for Passive Interference Nulling

Since the passive interference nulling presented in Sec. III-B achieves ZF when sufficient number of REs exist (typically $N \geq 2K - 1$), \mathbf{E} is a diagonal matrix. Hence, the transmission results in K virtual parallel streams. Therefore, full precoding is not required to maximize the sum rate. Alternatively, water-filling power allocation can be used, which is optimal for (25a). The closed-form water-filling solution is given as

$$p_k^* = \left(\frac{1}{\alpha} - \frac{N_0}{|\mathbf{h}_k^T \Theta^* \mathbf{w}_k|^2} \right)^+ \quad (26)$$

where α is the dual variable that can be found using bi-section search. It is worth noting that the water-filling solution for passive interference nulling converges to the uniform power solution at high signal to noise ratios (SNRs), unlike passive MRT which still requires power allocation/precoding at the BS. Hence, in the presence of imperfect CSI at high SNRs, passive interference nulling is more robust as CSI is only required at the BD-RIS, compared to passive MRT which requires CSI at the BS and BD-RIS.

V. NUMERICAL RESULTS AND DISCUSSIONS

This section presents the numerical results for the proposed two-stage designs as well as the benchmarks.

A. Simulation Setup

The adopted channel model is i.i.d Rayleigh fading with the distance-dependent large-scale fading given as $\Upsilon(d) = C_0 \left(\frac{d}{d_0}\right)^{-\rho}$, where d denotes the distance, $C_0 = -30$ dB denotes the reference pathloss, $d_0 = 1$ m is reference distance and $\rho = 2.2$ is the pathloss exponent. We consider the system to be operating at 2.4 GHz, with noise power spectral density $N_0 = -80$ dBm that is identical for all users. Unless otherwise stated, we consider the distance between BS and BD-RIS to be 50 m and the distance between the BD-RIS and users to be 2.5 m. We assume the channel state information to be known perfectly at the BS, BD-RIS and the users. For Algorithm 1, $\epsilon = 10^{-6}$, $\varepsilon = 10^{-6}$ and $\text{Iter} = 10^2$ are set. Hundred realizations are considered for Monte-Carlo simulation. The simulations were conducted on a work station equipped with 3.49 GHz 64 bits Apple M2 Pro chip with 12-core CPU and 16 GB RAM.

B. Notations for Proposed Designs and Benchmarks

Various *benchmarks* are used to compare the performance of our *proposed* designs for the BD-RIS. The notations for the *proposed* designs are given as follows:

- **BD-RIS MRT** denotes the passive MRT solution introduced in Sec. III-A.
- **BD-RIS Null** denotes the passive interference nulling introduced in Sec. III-B. Both random and MRT initializations are considered for Algorithm 1.

The notations for the processes at the BS are given as

- **UP** denotes the uniform power allocation shown in (24).
- **RM** denotes the rate maximization shown in (25a), (26).
- **ZF** denotes the zero-forcing shown in (23).

The *benchmarks* belong to two main categories: MIMO relays and RIS. Under MIMO relays, noiseless non-regenerative MIMO relays are considered with N -transmit, N -receive antennas and 36 dBm power budget operating in full-duplex without any self-interference. Two-stage design is considered:

- **nMIMO ZF** denotes performing ZF at the MIMO relay, while uniform power is performed at the BS. The computational complexity at the BS is negligible, whereas the computational complexity at the relay is $\mathcal{O}(N^3)$ which comes from computing the Moore-pseudoinverse of \mathbf{G} .
- **nMIMO MRT** denotes performing MRT at the MIMO relay, while ZF precoding is performed at the BS. The computational complexity at the relay is $\mathcal{O}(N^2)$ which comes from MRT computation based on \mathbf{G} .

D-RIS and BD-RIS are two RIS technologies that are considered. For D-RIS,

- **D-RIS Null** denotes interference nulling for D-RIS following [10].

Also, joint design and various two-stage designs are considered for BD-RIS:

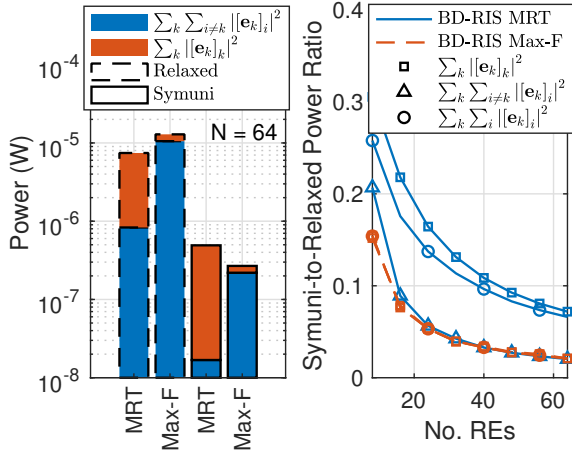


Fig. 3. Power and power ratio for BD-RIS considering **MRT** and **Max-F** for $p_k = 1, \forall k$ and $K = 5$.

- **BD-RIS Joint** denotes the joint-design following [18], which has a computational complexity of $\mathcal{O}(t_1 t_2 N^3)$ for $N \gg K$, where t_1 and t_2 are the number of iterations for the outer and inner loops.
- **BD-RIS Max-F** denotes the Frobenius norm-based maximum channel gain design for the BD-RIS scattering matrix. It aims to $\max_{\Theta} \|\mathbf{E}\|_F^2$, which has a relaxed closed-form solution that follows [28] and its symmetric unitary solution is given as $\Theta^* = \Pi_{\mathcal{S}_{\text{loss}}} \left(\Pi_{\mathcal{S}_{\text{recip}}} \left(\text{reshape} \left(\sqrt{N} \mathbf{v}_{\text{max}}, [N, N] \right) \right) \right)$, where \mathbf{v}_{max} is the Eigenvector of $\mathbf{A}^H \mathbf{A}$ associated with its dominant Eigenvalue. Its computational complexity comes from computing the SVD of an $N^2 \times N^2$ matrix and is $\mathcal{O}(N^6)$.
- **BD-RIS Max-l2** denotes the l^2 norm-based maximum channel gain design for the BD-RIS scattering matrix. It aims to $\max_{\Theta} \|\mathbf{E}\|_2^2$, which has a symmetric unitary solution that is described in [19]. Its computational complexity comes from computing the SVD of \mathbf{H} and \mathbf{W} and is $\mathcal{O}(N^3)$.
- **BS ZF** denotes the specular reflection by BD-RIS, i.e., $\Theta^* = \mathbf{I}$, where the BS performs ZF based on \mathbf{E} such that $\mathbf{P} = \mathbf{E}^\dagger \sqrt{\frac{P_{\text{max}}}{\text{Tr}(\mathbf{E}^H \mathbf{E})}}$ and has a computational complexity of $\mathcal{O}(K^3)$.
- **BS MRT** denotes the specular reflection by BD-RIS, i.e., $\Theta^* = \mathbf{I}$, where the BS performs MRT based on \mathbf{E} such that $\mathbf{P} = \mathbf{E}^H \sqrt{\frac{P_{\text{max}}}{\text{Tr}(\mathbf{E}^H \mathbf{E})}}$ and has a computational complexity of $\mathcal{O}(K^2)$.

Except for **nMIMO ZF** and **BS MRT**, the rest of the above mentioned two-stage designs consider performing ZF at the BS following (23), which has a computational complexity of $\mathcal{O}(K^3)$ that comes from computing the Moore-pseudoinverse of \mathbf{E} .

C. Simulation Results

Fig. 3 illustrates the received SINR at stage 1 of a BD-RIS with $K = 5$, comparing relaxed and symmetric unitary solutions for **BD-RIS MRT** and **BD-RIS Max-F**. Specifically, the figure breakdowns (5) into the sum of signal powers, sum

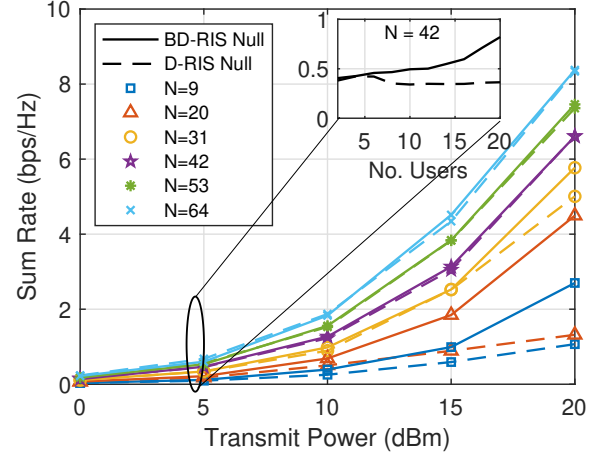


Fig. 4. Sum rate vs. transmit power for BD-RIS and D-RIS considering **Null** with random initialization, where $K = 5$ and $(2K - 1) \leq N \leq 2^{K+1}$.

of interference and Frobenius norm of the equivalent channel for $N = 64$ in a stacked bar chart. Also, it depicts the power ratio of the symmetric unitary solution to the relaxed solution. It is seen that the relaxed **BD-RIS Max-F** achieves the highest Frobenius norm having the highest bar. Nonetheless, the symmetric unitary solution for **BD-RIS Max-F** does not guarantee the maximization of the Frobenius norm as seen in the figure, where the symmetric unitary **BD-RIS MRT** is better. In addition, the sum of signal powers for the relaxed and symmetric unitary **BD-RIS MRT** are higher than that of **BD-RIS Max-F** as expected, whereas the sum of interference is higher for **BD-RIS Max-F** compared to **BD-RIS MRT** as the latter only maximizes the diagonal entries of the equivalent channel but the former maximizes all entries. Such observation indicates that **BD-RIS MRT** would have a better SINR at the users compared to **BD-RIS Max-F**. Furthermore, although the symmetric unitary projection degrades the sum of signal powers for both **BD-RIS Max-F** and **BD-RIS MRT**, it reduces the sum of interference for **BD-RIS MRT** at a higher rate such that the SINR can be effectively improved, unlike **BD-RIS Max-F** which reduces both the sum of signal powers and sum of interference at the same rate.

Fig. 4 compares the sum rate performance of AO to achieve interference nulling using BD-RIS and D-RIS [10]. Random initialization and uniform power allocation at the BS is assumed for both, where $K = 5$ and $(2K - 1) \leq N \leq 2^{K+1}$. It is shown that BD-RIS achieves better sum rate performance with a huge gap when $N = 2K - 1$, which is due to the fact that D-RIS needs $N > 2K(K - 1)$ to effectively achieve interference nulling with high probability. As N grows towards 2^{K+1} , the performance gap reduces accordingly, i.e., the performance gain of BD-RIS vanishes for $N > 2K(K - 1)$, which is justified as the interference is nulled for both BD-RIS and D-RIS considering the random initialization. This indicates other initialization points need to be investigated to show the BD-RIS performance gain over D-RIS. Furthermore, the snippet shows that for a given number of REs BD-RIS achieves an increasing sum rate by increasing K , unlike the D-RIS which achieves a reduced sum rate before saturation. This indicates that BD-RIS is a better candidate for interference nulling in

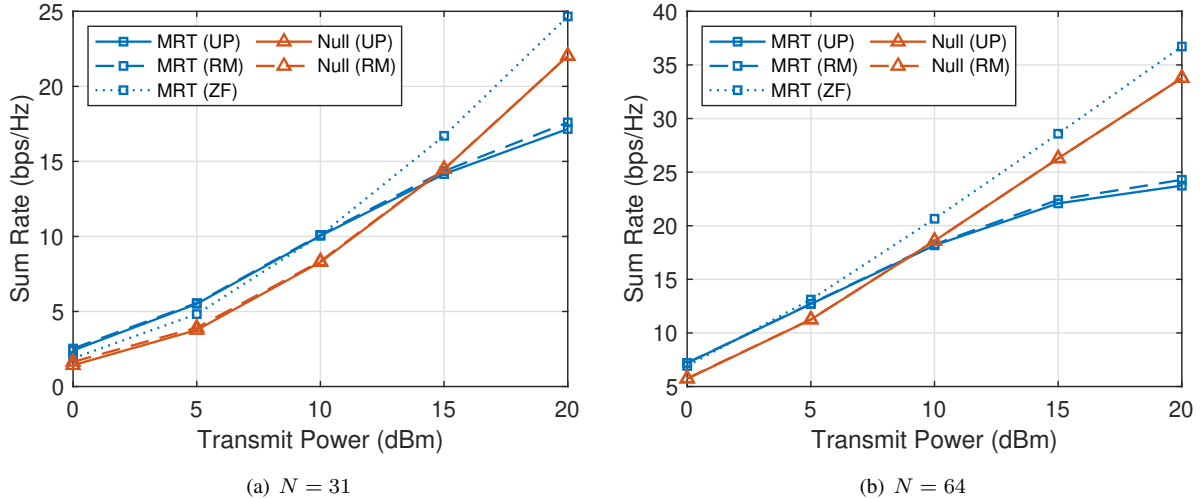


Fig. 5. Sum rate vs. transmit power for BD-RIS considering **Null** and **MRT**, where $K = 5$ and a) $N = 31$, b) $N = 64$.

dense MU-MISO due to its flexibility in designing Θ .

Fig. 5 shows the sum rate of BD-RIS vs. the transmit power at the BS. It considers the *proposed* BD-RIS designs. Specifically, **MRT** and **Null** with MRT initialization (14) are considered. Also, the impact of different BS processes are considered. The figure considers $K = 5$ users and $N \in \{31, 64\}$ REs. While focusing on **UP**, Fig. 5 shows that **MRT** enhances the sum rate at low SNRs, a regime in which the performance is dominated by noise. This is due to its better channel alignment compared to **Null**. Nonetheless, the performance of **MRT** is saturated at moderate and high SNRs due to being interference-limited, unlike **Null**. Such saturation is observed for smaller SNRs when the number of REs is increased since increasing the number of REs improves the SNR in general. On the other hand, **RM** power allocation schemes improve the sum rate in general. Moreover, **RM** improves the sum rate of **Null** slightly at low SNRs and small BD-RIS, whereas its improvement for high SNRs and large BD-RIS is negligible. Finally, **MRT** with **ZF** precoding at the BS outperforms **Null** with **RM** at the BS by ~ 3 dB at 20 bps/Hz. Hence, **MRT** with **ZF** at the BS maintains low computational complexity while achieving a good sum rate performance at low and moderate SNRs and the best sum rate performance at high SNRs.

Fig. 6 illustrates the sum rate for the *proposed* BD-RIS and the *benchmarks*, where $P_{\max} = 5$ dBm. In Fig. 6a, the sum rate is illustrated vs. the number of users, where $N = 5K$ REs. It can be seen that **BD-RIS Joint** serves as an upper bound for the sum rate for $N > 2$, where the gap increases as the number of users increase. This is justified because it optimizes both the scattering matrix of the BD-RIS and the precoding matrix at the BS simultaneously to maximize the sum rate unlike other *benchmarks* and *proposed* solutions. For instance, at $K = 10$, **BD-RIS Joint** achieves a sum rate of 14 bps/Hz, whereas **BD-RIS MRT** with **ZF** at the BS achieves a sum rate of 10.3 bps/Hz¹. Moreover, it is noted that **nMIMO** curves have

¹It is worth noting that the unitary constraint is only considered for **BD-RIS Joint** while the rest BD-RIS designs consider both symmetric and unitary constraints.

the same slope due to its limited power budget. Furthermore, **nMIMO ZF** achieves better sum rate than **nMIMO MRT** for such SNR. This is consistent with literature since the conventional **ZF** outperforms **MRT** at higher SNRs because **ZF** has the ability to minimize inter-user interference with slight power loss that is insignificant at such SNRs. Also, both *proposed* BD-RIS designs outperform **BD-RIS Max-F** and **BD-RIS Max-I2** designs because the *proposed* BD-RIS designs have better interference management in multiuser systems. In addition, **BS ZF** are both performing poorly since BD-RIS is not utilized to enhance the poor channel gains stemming from the double-fading effect. Therefore, relying solely on the BS for precoding becomes inefficient. For instance, **ZF** wastes most of the power for channel inversion leaving very small power gains. Moreover, the performance of the *proposed* designs improve as the number of users/REs increase which is justified as the scattering matrix Frobenius norm increases as well indicating their effectiveness in handling dense multiuser scenarios. While the gap between **BD-RIS MRT** and **BD-RIS Null** with MRT initialization increases as the number of users increase, the latter can be a good candidate to achieve a reasonable sum rate performance meanwhile maintaining a negligible complexity at the BS. Furthermore, Fig. 6b shows the sum rate vs. the number of REs for $K = 2$. It is seen that **nMIMO** curves achieve the best sum rate in this regime, while the specular reflection **BD-RIS** curves are both lower bounds and the justification holds from Fig. 6a. Furthermore, the gap between **BD-RIS Joint** and **BD-RIS MRT** is reduced significantly and it vanishes as the number of REs grows. This indicates that passive MRT with **ZF** precoding at the BS achieves local optimality while maintaining low complexity, and is considered a good candidate for BD-RIS with many REs. Also, the significance of **BD-RIS Max-F** and **BD-RIS Max-I2** is shown for high number of REs with an advantage for **BD-RIS Max-F**. Their poor performance with relatively small N is justified by the fact that the equivalent channel is ill-conditioned/poorly conditioned for such N values and it improves as N increases.

Fig. 7 shows the time complexity considering the *proposed*

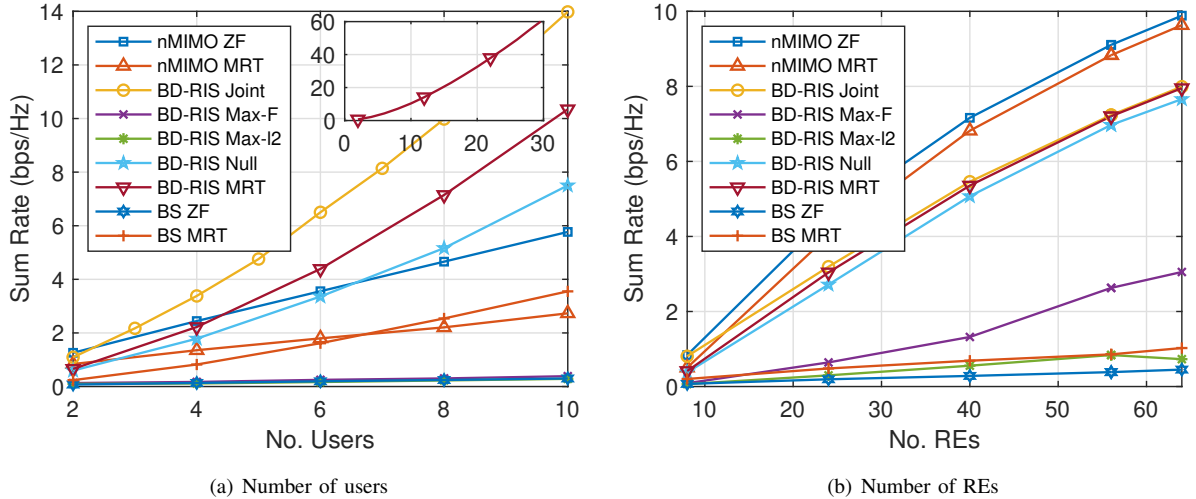


Fig. 6. Sum rate for the *benchmarks* and *proposed* BD-RIS designs with $P_{\max} = 5$ dBm. a) vs. number of users, $N = 5K$. b) vs. number of REs, $K = 2$.

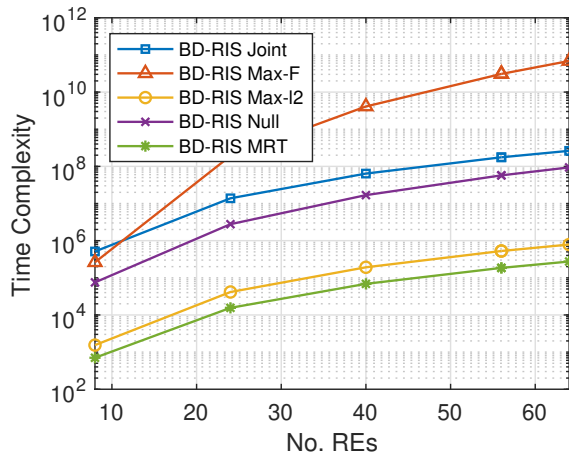


Fig. 7. Time complexity for the *benchmarks* and *proposed* BD-RIS designs with $P_{\max} = 5$ dBm vs. number of REs, $K = 2$.

BD-RIS and the *benchmarks*, where $K = 2$ and $P_{\max} = 5$ dBm. The worst-case scenario is considered for **BD-RIS Joint** and **BD-RIS Null** with MRT initialization, such that $t_1 = 50$, $t_2 = 20$, and $t = 100$. As presented in Sec. III and Sec. V-B, **BD-RIS MRT** has the lowest time complexity while the **BD-RIS Max-F** has the highest. In addition, **BD-RIS Max-I2** has a slightly higher time complexity than **BD-RIS MRT** because the former requires three SVD operations while the latter requires only one. Although **BD-RIS Joint** has a cubic time complexity, the complexity from the iterative algorithm is not negligible.

VI. CONCLUSIONS AND FUTURE WORK

To conclude, this work proposed a passive multiuser beamforming for BD-RIS-enabled MU-MISO systems. The passive multiuser beamforming designs are inspired by MRT and interference nulling. The former passive beamforming is presented in closed-form while the latter is presented in an AO framework. At the BS side, optimized/uniform power allocation and active precoding are considered. It is seen that BD-RIS reduces the number of REs required to achieve interference

nulling and achieves faster convergence compared to D-RIS. In addition, the passive MRT at BD-RIS with ZF precoding at the BS presents an effective low-complexity solution that simplifies channel estimation and achieves local optimality for MU-MISO scenarios with many REs.

For the future work, we will consider deriving a closed-form unitary symmetric scattering matrix to achieve *interference nulling* for the BD-RIS. In addition, we will analyze the average SINR and outage probability for the *passive MRT*. An extension to multi-antenna users will also be considered.

REFERENCES

- [1] M. Di Renzo *et al.*, "Smart radio environments empowered by reconfigurable intelligent surfaces: How it works, state of research, and the road ahead," *IEEE J. Sel. Areas Commun.*, vol. 38, no. 11, pp. 2450–2525, Nov. 2020.
- [2] —, "Reconfigurable intelligent surfaces vs. relaying: Differences, similarities, and performance comparison," *IEEE Open J. Commun. Soc.*, vol. 1, pp. 798–807, Jun. 2020.
- [3] J. An, C. Xu, L. Gan, and L. Hanzo, "Low-complexity channel estimation and passive beamforming for RIS-assisted MIMO systems relying on discrete phase shifts," *IEEE Trans. Commun.*, vol. 70, no. 2, pp. 1245–1260, Feb. 2022.
- [4] Y. Liu *et al.*, "Reconfigurable intelligent surfaces: Principles and opportunities," *IEEE Commun. Surveys Tuts.*, vol. 23, no. 3, pp. 1546–1577, 3rd Quart. 2021.
- [5] E. Björnson *et al.*, "Reconfigurable intelligent surfaces: A signal processing perspective with wireless applications," *IEEE Signal Process. Mag.*, vol. 39, no. 2, pp. 135–158, Feb. 2022.
- [6] Q. Wu and R. Zhang, "Intelligent reflecting surface enhanced wireless network via joint active and passive beamforming," *IEEE Trans. Wireless Commun.*, vol. 18, no. 11, pp. 5394–5409, Nov. 2019.
- [7] Z. Yang, W. Xu, C. Huang, J. Shi, and M. Shikh-Bahaei, "Beamforming design for multiuser transmission through reconfigurable intelligent surface," *IEEE Trans. Commun.*, vol. 69, no. 1, pp. 589–601, Jan. 2021.
- [8] Q.-U.-A. Nadeem *et al.*, "Intelligent reflecting surface-assisted multiuser MISO communication: Channel estimation and beamforming design," *IEEE Open J. Commun. Soc.*, vol. 1, pp. 661–680, May 2020.
- [9] Y. Liu, L. Zhang, and M. A. Imran, "Multi-user beamforming and transmission based on intelligent reflecting surface," *IEEE Trans. Wireless Commun.*, vol. 21, no. 9, pp. 7329–7342, Sep. 2022.
- [10] T. Jiang and W. Yu, "Interference nulling using reconfigurable intelligent surface," *IEEE J. Sel. Areas Commun.*, vol. 40, no. 5, pp. 1392–1406, May 2022.
- [11] F. Zhu *et al.*, "Robust beamforming for RIS-aided communications: Gradient-based manifold meta learning," *arXiv preprint arXiv:2402.10626*, 2024.

- [12] S. Jangsher, M. Al-Jarrah, A. Al-Dweik, E. Alsusa, and P.-Y. Kong, "Energy constrained sum-rate maximization in IRS-assisted UAV networks with imperfect channel information," *IEEE Trans. Aerosp. Electron. Syst.*, vol. 59, no. 3, pp. 2898–2908, Jun. 2023.
- [13] S. Shen, B. Clerckx, and R. Murch, "Modeling and architecture design of reconfigurable intelligent surfaces using scattering parameter network analysis," *IEEE Trans. Wireless Commun.*, vol. 21, no. 2, pp. 1229–1243, Feb. 2022.
- [14] H. Li, S. Shen, M. Nerini, and B. Clerckx, "Reconfigurable intelligent surfaces 2.0: Beyond diagonal phase shift matrices," *IEEE Commun. Mag.*, vol. 62, no. 3, pp. 102–108, Mar. 2024.
- [15] M. Nerini, S. Shen, H. Li, and B. Clerckx, "Beyond diagonal reconfigurable intelligent surfaces utilizing graph theory: Modeling, architecture design, and optimization," *IEEE Trans. Wireless Commun.*, pp. 1–1, 2024.
- [16] Q. Li *et al.*, "Reconfigurable intelligent surfaces relying on non-diagonal phase shift matrices," *IEEE Trans. Veh. Technol.*, vol. 71, no. 6, pp. 6367–6383, Jun. 2022.
- [17] T. Fang and Y. Mao, "A low-complexity beamforming design for beyond-diagonal RIS aided multi-user networks," *IEEE Commun. Lett.*, vol. 28, no. 1, pp. 203–207, Jan. 2024.
- [18] H. Li, S. Shen, and B. Clerckx, "Beyond diagonal reconfigurable intelligent surfaces: A multi-sector mode enabling highly directional full-space wireless coverage," *IEEE Trans. Wireless Commun.*, vol. 41, no. 8, pp. 2446–2460, Aug. 2023.
- [19] M. Nerini, S. Shen, and B. Clerckx, "Closed-form global optimization of beyond diagonal reconfigurable intelligent surfaces," *IEEE Trans. Wireless Commun.*, vol. 23, no. 2, pp. 1037–1051, Feb. 2024.
- [20] Z. Liu, Y. Liu, S. Shen, Q. Wu, and Q. Shi, "Enhancing ISAC network throughput using beyond diagonal RIS," *IEEE Wireless Commun. Lett.*, vol. 13, no. 6, pp. 1670–1674, Jun. 2024.
- [21] K. Chen and Y. Mao, "Transmitter side beyond-diagonal RIS for mmWave integrated sensing and communications," *arXiv preprint arXiv:2404.12604*, 2024.
- [22] I. Santamaria, M. Soleymani, E. Jorswieck, and J. Gutiérrez, "SNR maximization in beyond diagonal RIS-assisted single and multiple antenna links," *IEEE Signal Process. Lett.*, vol. 30, pp. 923–926, 2023.
- [23] R. Zhang, C. C. Chai, and Y.-C. Liang, "Joint beamforming and power control for multiantenna relay broadcast channel with QoS constraints," *IEEE Trans. Signal Process.*, vol. 57, no. 2, pp. 726–737, Feb. 2009.
- [24] E. Björnson, M. Bengtsson, and B. Ottersten, "Optimal multiuser transmit beamforming: A difficult problem with a simple solution structure [lecture notes]," *IEEE Signal Process. Mag.*, vol. 31, no. 4, pp. 142–148, Jul. 2014.
- [25] T. Lo, "Maximum ratio transmission," *IEEE Trans. Commun.*, vol. 47, no. 10, pp. 1458–1461, Oct. 1999.
- [26] X. Tang and Y. Hua, "Optimal design of non-regenerative MIMO wireless relays," *IEEE Trans. Wireless Commun.*, vol. 6, no. 4, pp. 1398–1407, Apr. 2007.
- [27] E. Björnson, D. Hammarwall, and B. Ottersten, "Exploiting quantized channel norm feedback through conditional statistics in arbitrarily correlated MIMO systems," *IEEE Trans. Signal Process.*, vol. 57, no. 10, pp. 4027–4041, Oct. 2009.
- [28] O. T. Demir and E. Björnson, "Is channel estimation necessary to select phase-shifts for RIS-assisted massive MIMO?" *IEEE Trans. Wireless Commun.*, vol. 21, no. 11, pp. 9537–9552, Nov. 2022.
- [29] H. Li, S. Shen, Y. Zhang, and B. Clerckx, "Channel estimation and beamforming for beyond diagonal reconfigurable intelligent surfaces," *IEEE Trans. Signal Process.*, vol. 72, pp. 3318–3332, 2024.
- [30] J. An, M. Di Renzo, M. Debbah, and C. Yuen, "Stacked intelligent metasurfaces for multiuser beamforming in the wave domain," in *IEEE Int. Conf. Commun. (IEEE ICC)*, Rome, Italy, 2023, pp. 2834–2839.
- [31] C. Huang, A. Zappone, G. C. Alexandropoulos, M. Debbah, and C. Yuen, "Reconfigurable intelligent surfaces for energy efficiency in wireless communication," *IEEE Trans. Wireless Commun.*, vol. 18, no. 8, pp. 4157–4170, Aug. 2019.